Journal of Alloys and Compounds, 213/214 (1994) 61–66
JALCOM 4104

Observation of enhanced nuclear stability near the 162 neutron shell

R.W. Lougheed, K.J. Moody, J.F. Wild, E.K. Hulet and J.H. McQuaid
University of California, Lawrence Livermore National Laboratory, Berkeley, CA 94551 (USA)

Yu.A. Lazarev, Yu.V. Lobanov, Yu.Ts. Oganessian, V.K. Utyonkov, F.Sh. Abdullin, G.V. Buklanov, B.N. Gikal, S. Iliev, A.N. Mezentsev, A.N. Polyakov, I.M. Sedykh, I.V. Shirokovsky, V.G. Subbotin, A.M. Sukhov, Yu.S. Tsyganov and V.E. Zhuchko
Joint Institute for Nuclear Research, 141980 Dubna (Russian Federation)

Abstract

In bombardments of ^{248}Cm with ^{22}Ne we discovered two new isotopes, ^{265}106 and ^{266}106, by establishing genetic links between α decays of the 106 nuclides and spontaneous fission (SF) or α decays of the daughter (or grand-daughter) nuclides. For ^{266}106 we measured $E_\alpha = 8.63 \pm 0.05$ MeV followed by the SF decay of ^{262}104 for which we measured a half-life value of $1.2^{+1.0}_{-0.5}$ s. For ^{265}106 we measured $E_\alpha = 8.71$–8.91 MeV. We estimated α half-lives of 10–30 s for ^{266}106 and 2–30 s for ^{265}106 with SF branches of approximately 50% or less. The decay properties of ^{266}106 indicate a large enhancement in the SF stability of this N = 160 nuclide and confirm the existence of the predicted deformed shells N = 162 and Z = 108.

1. Introduction

Recent calculations that include the predicted deformed neutron shell at N = 162 and the proton shell at Z = 108 indicate that nuclides in this region may have considerably greater stability against spontaneous fission (SF) than previously thought. Yet other recent calculations that also include the deformed shells lead to the opposite conclusion: a decrease in the stability against SF. Increased stability near N = 162 and Z = 108 was predicted using macroscopic–microscopic calculations which included larger deformation spaces [1–3]. For nuclei near Z = 108 and N = 162, T_{sf} values of tens of years were calculated. A decrease in stability was predicted by Möller *et al.* [4–7] using macroscopic–microscopic calculations, which showed a deep second fission valley leading to very compact scission shapes close to the fragment magic numbers $Z = 2 \times 50$ and $N = 2 \times 82$. SF half-lives were predicted to be very short because the second valley is lower in energy making the fission barrier "thinner", and because the inertia along the new path is greatly decreased. Thus the stabilizing effect of the N = 162 and Z = 108 shells is canceled by the destabilizing effect of the new valley, and the T_{sf} values are closer to milliseconds. This competition between features of the SF process which lead to such large differences in stability makes experiments that explore ground-state decay properties of nuclei around N = 162 one of the most important tasks in heavy element research.

We wanted to produce an even–even nuclide near these deformed shells because the decay of odd–odd or odd–mass nuclides can be strongly hindered by single particle effects, making it more difficult to compare their decay properties with theory. Among the heavy known even–even nuclides, ^{264}108 (N = 156) and ^{260}106 (N = 154) are too far from N = 162. The SF-decaying nuclide ^{262}104 (N = 158) was tentatively assigned a half-life value of about 50 ms [8, 9]; this half-life value still does not allow us to choose between the two predictions. A hint of increased stability against SF does come from the decay properties of ^{262}102, the only known nuclide with N = 160, which decays by SF with T_{sf} of about 5 ms [10]. However this nuclide is too low in Z to feel any influence of the predicted Z = 108 shell.

We report here on our experiments resulting in the first direct evidence of nuclear stability near the predicted deformed shell N = 162 and Z = 108 by producing the N = 160 nuclide ^{266}106 and also ^{265}106 using the fusion–evaporation reaction ^{248}Cm + ^{22}Ne. Prior to our work, four isotopes of element 106 had been identified. These are the odd-A α-emitters ^{259}106 [11], ^{261}106 [11], and ^{263}106 [12] with half-lives in the range 0.3–0.9 s,

0925-8388/94/$07.00
SSDI 0925-8388(94)04104-C

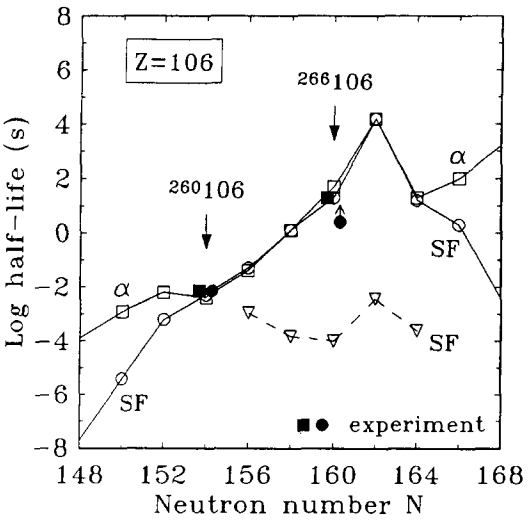

Fig. 1. Predicted partial half-lives for SF decay and α decay [3] of the even–even 106 isotopes shown by the lines connecting circles and squares, respectively. The dashed line connecting the triangular points shows T_{sf} calculations [4] which include the destabilizing effect of the predicted new fission valley. The filled points at ^{260}106 which are close to the calculated points are experimental values for both SF and α decay.

as well as the 3.6 ms even–even isotope ^{260}106 [11, 13, 14] which has an SF branch of 50^{+30}_{-20}%.

The ground-state decay properties of ^{266}106 should be a quite sensitive probe of the theoretical predictions in Fig. 1. If there is increased stability near N = 162 and Z = 108, the isotope ^{266}106 should have an SF- or α-decay half-life of tens of seconds. If there is decreased stability, ^{266}106 should decay by SF with a half-life of about 100 μs, a T_{sf} difference of a factor of about 10^5. Thus a distinct signature for enhanced nuclear stability near N = 162 would be the observation of ^{266}106 decay by α particle emission followed shortly by the SF decay of the daughter nucleus ^{262}104. A signature for the odd-A isotope ^{265}106, would be the observation of ^{265}106 α decay followed by α decays of the well-known daughter and grand-daughter α emitters ^{261}104 and ^{257}102.

2. Experimental details

We used the fusion–evaporation reaction ^{248}Cm + ^{22}Ne (116 and 121 MeV bombarding energies) to produce the new isotopes ^{265}106 and ^{266}106. We also performed periodic bombardments of ^{197}Au + ^{22}Ne for calibration and test purposes as well as a 1-day calibration run using the ^{235}U + ^{22}Ne reaction to measure the SF activity from the known nuclide, ^{252}102. Beams of ^{22}Ne projectiles from the U400 cyclotron of the Joint Institute for Nuclear Research passed through a rotating Ti entrance-window which separated the cyclotron vacuum from the hydrogen atmosphere of the targets and a gas-filled separator. Three ^{248}Cm targets were arranged on the periphery of a target wheel which was rotated synchronously with the 150 Hz frequency of the U400 cyclotron so that a target was exposed to the approx. 2.2 ms beam macropulse (inbeam) during each 6.7 ms beam cycle. The target wheel contained about 2.77 mg of ^{248}Cm deposited on a total area of 11.7 cm^2 (237 μg cm^{-2} average). The ^{248}Cm targets (approx. 97% ^{248}Cm and 3% ^{246}Cm) were prepared by multiple electrodepositions of Cm nitrate from an isobutanol solution onto 0.71 mg cm^{-2} Ti foils. The surface of the targets was covered by a 30 ± 5 μm cm^{-2} carbon layer. The same three ^{248}Cm targets were used during the 16-day bombardments with typical intensities of 1.5×10^{13} pps of ^{22}Ne and a total fluence of about 1.6×10^{19} particles of ^{22}Ne.

Evaporation residues (EVRs) recoiling out of the ^{248}Cm targets were separated in-flight from beam particles and transfer products by the gas-filled recoil separator which is described in Refs. 15–17. We set the magnetic rigidity value of the separator for the Z = 106 EVRs based on measurements of the average charge state in hydrogen for the slow EVRs with Z = 100, 102 and 104 made in the reactions ^{235}U + ^{18}O, ^{235}U + ^{22}Ne, and ^{242}Pu + ^{22}Ne [17, 18]. The separated EVRs passed a time-of-flight (TOF) counter composed of pair of large-area multiwire proportional chambers placed in a 1 Torr pentane-filled module before impinging onto a position-sensitive surface-barrier detector (PSD).

The PSD counting array consisted of three surface-barrier detectors with each detector having eight 40×4.8 mm strips. The three detectors were placed in the focal plane of the separator to form a 124×40 mm array with the individual strips oriented in the 40 mm vertical direction. The detectors were made from P type (instead of the usual N type) silicon with N^+ diffusions on the front surface (implant side) and boron implanted on the back surface to form the resistive layer [19]. Signals from the detector strips were processed for α and implant energies (approx. 0.5–15 MeV). Top and bottom signals from the back surface of the detectors were split into two channels to provide position signals for α/implant events (approx. 0.5–15 MeV) and fission events (15–200 MeV). We calculated total fission energies by summing the position energy signals. Gate signals were generated by summing fast signals from each detector. With each recorded event, we recorded several additional parameters including the strip number, TOF information, beam current, beam pulse number, the time in microseconds from beginning of the beam pulse to either α/implant or fission events, and the time since the beginning of the data acquisition cycle in 0.1 ms intervals.

The data were stored in list mode in an LSI 11/73 computer and were transferred periodically using a general-purpose instrument bus from the LSI 11/73 to a microVAX II computer for permanent storage and subsequent off-line analysis.

Energy calibration were performed for each strip using the α peaks from nuclides produced in the $^{197}Au + ^{22}Ne$ calibration reactions. The reproducibility of the calibrations was ~20 keV with most of the strips having energy resolutions of 95–120 keV. An approximate fission energy calibration was based on an extrapolation of the α-energy calibration and by setting the separator magnetic rigidity so that approximately full-energy ^{22}Ne projectiles impinged on the detectors. We used known α–α, EVR–α, and EVR–SF decay sequences from the calibration reactions to estimate full-width at half maximum position resolutions of approx. 3% of the strip length for the α–α decay sequences and approx. 9% for α-SF or EVR–α decay sequences.

We had low efficiencies for detecting EVRs or α particles escaping the detectors due to low EVR implantation energies. The initial Z = 106 EVR energy of 7 MeV was reduced to less than 1 MeV detected energy in the PSDs by losses in the target, hydrogen gas, the TOF module, the detector dead layer, and plasma effects in the detector. This resulted in most of the EVR and α escape signals being below the detection threshold and prevented us from efficiently detecting correlated EVR–α and EVR–SF decay chains, and α–SF or α–α decay chains when one of the α particles escaped the detector.

In the off-line analyses we searched for time correlations between α and α or SF events. The out-of-beam background at the α energies (Fig. 2) of interest and SF events (Fig. 3) was so low, about one event per day per strip, that vertical position correlation criteria were not needed to establish out-of-beam correlations occurring within tens of minutes. We could distinguish in-beam α–SF correlations from random correlations at time intervals of tens of seconds by using a ±10% vertical position criterion.

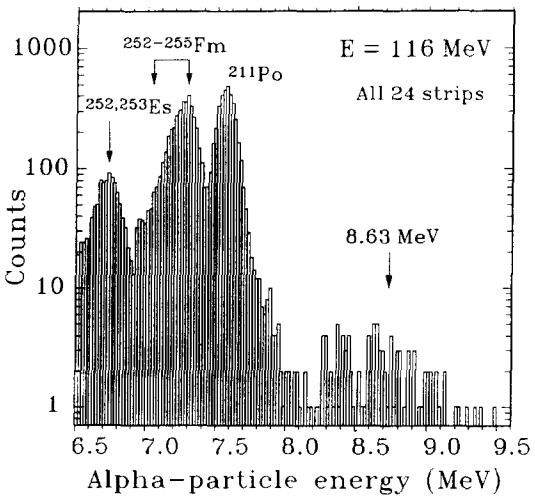

Fig. 2. Out-of-beam α-energy spectrum for all 24 strips.

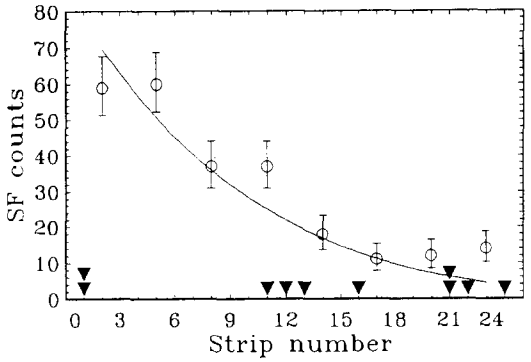

Fig. 3. Out-of-beam SF events vs. detector location at 116 MeV. Each three adjacent strips are summed together. The smooth curve is a fit to the distribution across the strips of the Fm α-events shown in Fig. 2. The filled triangles show the location of α–α–(α) and α-SF correlations from both the 116 and 121 MeV bombardments.

3. Results

In Table 1 we show the α–SF and α–α–(α) correlations for the 116 MeV and 121 MeV bombardments. Table 2 shows the production cross-sections, α energies, and half-life estimates for $^{265}106$ and $^{266}106$.

We attribute the six α-SF event pairs at 116 MeV and 121 MeV (Table 1) with $E_\alpha = 8.63 \pm 0.05$ MeV to the decay chain $^{266}106 \rightarrow ^{262}104$ for which we measured a production cross-section of 80 pb at 116 MeV and 60 pb at 121 MeV. We assigned the four α–α–(α) correlations at 121 MeV with $E_{\alpha 1} = 8.71$–8.91 MeV to the decay chain $^{265}106 \rightarrow ^{261}104$ ($T_{1/2} = 65$ s, $E_\alpha \approx 8.29$ MeV) $\rightarrow ^{257}104$ ($T_{1/2} = 26$ s, $E_\alpha \approx 8.22$, 8.27, 8.32 MeV) for which we measured a production cross-section of 260 pb. We attribute the last α–α (8.16 and 8.17 MeV) correlation shown in Table 1 to the decay chain $^{261}104 \rightarrow ^{257}104$.

Our assignment of the six α-SF correlations to the decay of $^{266}106$ is based on the following observations. The observed α-SF correlation chains with $E_\alpha = 8.63$ MeV and short correlation times in the range 0.2–6.4 s are unique: we cannot identify any candidate α-SF pairs with other Z,A values which would have similar decay properties. The observed α energy is in agreement with predictions as is the expectation of SF decay by an even–even Z = 104 daughter. The six α-SF correlation chains were detected by using a gas-filled recoil separator which strongly suppresses many kinds of background reaction products while collecting compound nucleus products. The α-SF and α–α chains were broadly dis-

TABLE 1. Parameters of the α–α and α–SF correlation chains observed in the $^{248}Cm+^{22}Ne$ reaction. The quoted SF energies are measured values; no estimate was included for the pulse-height defect on the fraction of the total kinetic energy deposited in the detectors

Decay mode	Particle energy (MeV)	Strip number	Time interval	Position deviation		Beam-pulse
				%	mm	
Bombarding energy 116 MeV						
α	8.60	16				off
SF	105	16	191 ms	−7.6	−3.0	off
α	8.54	22				off
SF	89	22	215 ms	7.4	3.0	off
α	8.59	24				off
SF	96	24	748 ms	3.3	1.3	off
α	8.74	21				off
SF	118	21	6453 ms	−4.5	−1.8	off
Bombarding energy 121 MeV						
α	8.69	11				on
SF	103	11	360 ms	−0.8	−0.3	on
α	8.60	13				on
SF	118	13	2011 ms	4.5	1.8	off
α	8.85	21				off
α	8.20	21	3 s	2.0	0.8	off
α	8.81	1				off
α	8.31	1	334 s	0.8	0.3	off
α	8.17	1	60 s	−2.6	−1.0	off
α	8.91	1				off
α	8.12	1	86 s	?	?	off
α	8.71	12				off
α	8.14	12	20 s	−0.6	−0.2	off
α	8.16	8				off
α	8.17	8	1 s	1.8	0.7	off

TABLE 2. Production cross-sections and decay properties of for the new Z=106 nuclides

Isotope	Cross-section (pb)[a]	Half-life (s)	E_α (MeV)
$^{265}106$	121 MeV:260	2–30[b]	8.71–8.91
$^{266}106$	116 MeV:80 121 MeV:60	10–30	8.63±0.05

[a]The cross sections are reported with an estimated accuracy of a factor of approximately 3.
[b]Assuming a hindrance factor of 1–3.

tributed across the detector strips as expected for a compound nucleus reaction, while the largest number of single SF and α events, which come from transfer products like ^{256}Fm and lighter Fm isotopes, occurred in the lower numbered strips. Finally, the production cross-sections for $^{266}106$ at both 116 and 121 MeV agree with systematics.

We assigned four α–α correlations to the decay of $^{265}106$ using similar arguments to those given above for $^{266}106$. Especially convincing is detection of the triple α–α–α correlation in which we observed both the Z=104 and Z=102 α-decay daughters following an 8.81 MeV α particle. In addition, we did not observe any α–α correlations at the 116 MeV bombarding energy which is below the $^{248}Cm(^{22}Ne,5n)$ reaction threshold. We note that except for the one triple correlation, due to their similar α energies and half-lives, we cannot distinguish between the αs from $^{261}104$ and from $^{257}102$.

The above points provide consistent evidence for the assignment of the observed correlation chains to the α decay of $^{265}106$ and $^{266}106$. The correlation times for the α-SF chains give a half-life of $1.2^{+1.0}_{-0.5}$ s (Fig. 4) rather than the half-life of 47 ms that was tentatively assigned by Somerville *et al.* [8, 9] to $^{262}104$. We argue that $^{262}104$ decays with an SF half-life of about 1.2 s based on our observations and that this assignment is consistent with the observations of Somerville *et al.* [8, 9]. Both 1.3 s and 47 ms SF activities were produced by Somerville *et al.* [8, 9] at the near-barrier bombarding energies 89 MeV and 95 MeV in the $^{248}Cm+^{18}O$ reaction. Hoffman *et al.* [20] also produced a 1.5 s activity and measured its fission properties in the $^{248}Cm+^{18}O$ reaction at 95 MeV. Our interpretation of Somerville's work is that both the 1.3 s and 47 ms activities are candidates for $^{262}104$ and that our observations establish that the 1.3 s activity is from the ground-state decay of $^{262}104$. The possibility that the 47 ms SF activity is associated with the presence of a quasiparticle K-isomeric state in $^{262}104$ is discussed in Ref. 17.

Before comparing our results with theoretical predictions we need to estimate the ground-state decay properties of $^{265}106$ and $^{266}106$. Because we did not have the efficiency to observe EVRs preceding α or SF events, we have to estimate the partial α-decay half-lives from the α-decay energies, and the SF branching

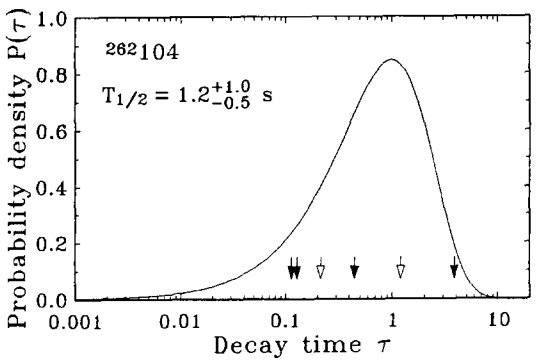

Fig. 4. The probability density function for the six α-SF correlations vs. the decay time. Solid arrows are the correlations from the 116 MeV bombardments and open arrows are the correlations from the 121 MeV bombardments.

ratios from background rates and cross-section measurements.

Because $^{266}106$ is even–even, its α decay will be ground state to ground state and the estimation of its α half-life is straightforward. Using the semiempirical formula of Viola and Seaborg quoted in Ref. 2 and the measured α energy, we estimate the partial α half-life of $^{266}106$ to be between 10 and 30 s. Similarly, we estimate an α half-life of 2–30 s for $^{265}106$ assuming a hindrance factor of 1–3.

The α-branching ratios are probably $\geqslant 50\%$ for both 106 nuclides based on our cross-section measurements which are about the expected values for the 4n and 5n channels. We calculated a very conservative α-branching limit of $>15\%$ for $^{266}106$ from the beam-off data at 116 MeV by assuming that all of the observed fissions in the higher numbered strips are from $^{266}106$ SF decay or the SF decay of its daughter, $^{262}104$. Most of the observed SF events are actually from the transfer product ^{256}Fm, based on their distribution across the strips and on their yield compared to the yield of α-emitting Fm isotopes [21].

4. Discussion and conclusions

The relatively long α half-life and the SF half-life limit for $^{266}106$ are in good agreement with the predictions of increased stability [1–3] near $N=162$. Our new SF half-life value for $^{262}104$, 1.2 s, is somewhat longer than the 0.25 s predicted by Sobiczewski [3]. The short SF half-lives predicted by Möller *et al.*, which are based on a thinner fission barrier and a lower inertia SF path, are inconsistent with our results. Since the "new valley" calculated by Möller *et al.* [22–24] has been shown to exist, at least up to $Z=102$, our results indicate that the inertia leading to the new valley is not low enough to cause a significant reduction in the increased stability caused by the deformed neutron shell at $N=162$ and proton shell at $Z=108$.

The conclusion that the increased stability of $^{266}106$ is caused by its nearness to $N=162$ and $Z=108$ means that stability against SF will be even greater if nuclides closer to or exactly at these shells can be made. A brief discussion of these possibilities is given in Ref. 17. Neutron numbers from 160 to as high as 166 at $Z=110$ can be made using various combinations of ^{32,34,36}S bombardments of ^{242,244}Pu. Alpha decay of these nuclides would lead to unknown nuclides of element 108 with neutron numbers as high as 164.

The tens of seconds half-lives for these new nuclides create new opportunities for studying the chemistry of element 106; previously the longest-lived 106 nuclide had a 0.9 s half-life.

Acknowledgments

We thank the U400 cyclotron staff for providing long-term bombardments with intense ^{22}Ne beams. We thank V.V. Bekhterev, V.I. Krashonkin, I.V. Kolesov, the late V.M. Plotko, L.I. Salamatin, D.H. Tinoco, J.T. Walton and E.D. Watkins for their essential help. Three of us (RWL, KJM, and JFW) would like to thank the Joint Institute for Nuclear Research for their hospitality during the course of the experiments at JINR. The curium target material supplied by the Livermore collaborators was provided by the Office of Basic Energy Sciences, US. Department of Energy, through the transplutonium production facilities of the Oak Ridge National Laboratory. Most of the support for the Livermore collaborators was provided through the US Department of Energy by the Lawrence Livermore National Laboratory under contract No. W-7405-Eng-48.

References

1 Z. Patyk and A. Sobiczewski, *Phys. Lett. B, 256* (1991) 307.
2 Z. Patyk and A. Sobiczewski, *Nucl. Phys. A, 533* (1991) 132.
3 A. Sobiczewski, *J. Alloys Comp., 213/214* (1994) 38.
4 P. Möller, J.R. Nix and W.J. Swiatecki, *Nucl. Phys. A, 492* (1989) 349.
5 P. Möller and J.R. Nix, *Nucl. Phys. A, 549* (1992) 84.
6 P. Möller, these proceedings.
7 P. Möller, J.R. Nix and W.J. Swiatecki, *Nucl. Phys. A, 469* (1987) 1.
8 L.P. Somerville, M.J. Nurmia, J.M. Nitschke, A. Ghiorso, E.K. Hulet and R.W. Lougheed, *Phys. Rev. C, 31* (1985) 1801.
9 L.P. Somerville, *Ph.D. Thesis,* University of California, Berkeley, Lawrence Berkeley Laboratory Report No. LBL-14050, 1982.
10 R.W. Lougheed, E.K. Hulet, J.F. Wild, K.J. Moody, R.J. Dougan, C.M. Gannett, R.A. Henderson, D.C. Hoffman and D.M. Lee, *Fifty Years with Nuclear Fission,* Vol. 2, American Nuclear Society, La Grange Park, IL, 1989, p. 694.
11 G. Münzenberg, S. Hofmann, H. Folger, F.P. Hessberger, J. Keller, K. Poppensieker, B. Quint, W. Reisdorf, K.H. Schmidt, H.J. Schött, P. Armbruster, M.E. Leino and R. Hingmann, *Z. Phys. A, 322* (1985) 227.
12 A. Ghiorso, J.M. Nitschke, J.R. Alonso, C.T. Alonso, M. Nurmia, G.T. Seaborg, E.K. Hulet and R.W. Lougheed, *Phys. Rev. Lett., 33* (1974) 1490.
13 Yu.Ts. Oganessian, Yu.P. Tretyakov, A.S. Iljinov, A.G. Demin, A.A. Pleve, S.P. Tretyakova, V.M. Plotko, M.P. Ivanov, N.A. Danilov, Yu.S. Korotkin and G.N. Flerov, *Zh. Eksperim. Theor. Fiz. Pis'ma, 20* (1974) 580 [*Sov. JETP Lett., 20* (1974) 265.
14 A.G. Demin, S.P. Tretyakova, V.K. Utyonkov and I.V. Shirokovsky, *Z. Phys. A, 315* (1984) 197.
15 Yu.Ts. Oganessian, Yu.V. Lobanov, A.G. Popeko, J. Rigol, F.Sh. Abdullin, V.V. Bekhterev, G.G. Gulbekyan, A.A. Ledovskoy, V.N. Melnikov, S.P. Tretyakova, Yu.P. Kharitonov, Yu.S. Tsyganov and V.A. Chugreev, in *Proc. Int. School-Seminar on Heavy Ion Physics, Dubna, 1989,* Joint Institute for Nuclear Research Report No. D7-90-142, 1990, p. 44.

16 Yu.A. Lazarev, Yu.V. Lobanov, A.N. Mezentsev, Yu.Ts. Oganessian, V.G. Subbotin, V.K. Utyonkov, F.Sh. Abdullin, V.V. Bekhterev, S. Iliev, I.V. Kolesov, A.N. Polyakov, I.M. Sedykh, I.V. Shirokovsky, A.M. Sukhov, Yu.S. Tsyganov and V.E. Zhuchko, in *Heavy Ion Physics, Scientific Report 1991–1992*, Joint Institute for Nuclear Research, Dubna, Report No. E7-93-57, 1993, p. 203; in *Proc. Int. School-Seminar on Heavy Ion Physics, Dubna, 1993,* JNIR Report No. E7-93-274, 1993, Vol. 2, p. 497.

17 Yu.Ts. Oganessian, *J. Alloys Comp., 213/214* (1994) 50.

18 Yu.A. Lazarev, Yu.V. Lobanov, Yu.Ts. Oganessian, Yu.S. Tsyganov, V.K. Utyonkov, F.Sh. Abdullin, G.V. Buklanov, B.N. Gikal, S. Iliev, A.N. Mezentsev, A.N. Polyakov, I.M. Sedykh, I.V. Shirokovsky, V.G. Subbotin and A.M. Sukhov, in *Heavy Ion Physics, Scientific Report 1991–1992,* Joint Institute for Nuclear Research, Dubna, Report No E7-93-57, 1993, p. 39.

19 J.T. Walton and F.S. Goulding, *IEEE Trans. Nuclear Sci., NS-34* (1987) 396.

20 D.C. Hoffman, D.Lee, A. Ghiorso, M.J. Nurmia, K. Aleklett and M. Leino, *Phys. Rev. C, 24* (1981) 495.

21 D. Lee, H.R. von Gunten, B. Jacak, M. Nurmia, Y.-F. Liu, C. Luo, G.T. Seaborg and D.C. Hoffman, *Phys. Rev. C, 25* (1982) 286.

22 E.K. Hulet, J.F. Wild, R.J. Dougan, R.W. Lougheed, J.H. Landrum, A.D. Dougan, M. Schädel, R.L. Hahn, P.A. Baisden, C.M. Henderson, R.J. Dupzyk, K. Sümmerer and G.R. Bethune, *Phys. Rev. Lett., 56* (1986) 313.

23 E.K. Hulet, in *Proc. Robert A. Welch Foundation Conference on Chemical Research XXXIV "Fifty Years with Transuranium Elements", Houston, TX, 1990,* p. 279.

24 E.K. Hulet, J.F. Wild, R.J. Dougan, R.W. Lougheed, J.H. Landrum, A.D. Dougan, P.A. Baisden, C.M. Henderson, R.J. Dupzyk, R.L. Hahn, M. Schädel, K. Sümmerer and G.R. Bethune, *Phys. Rev. C, 40* (1989) 770.